

# UCSF

## UC San Francisco Previously Published Works

### Title

Targeted polypharmacology: discovery of dual inhibitors of tyrosine and phosphoinositide kinases

### Permalink

<https://escholarship.org/uc/item/70c0785z>

### Journal

Nature Chemical Biology, 4(11)

### ISSN

1552-4450

### Authors

Apsel, Beth  
Blair, Jimmy A  
Gonzalez, Beatriz  
[et al.](#)

### Publication Date

2008-11-01

### DOI

10.1038/nchembio.117

Peer reviewed



Published in final edited form as:

*Nat Chem Biol.* 2008 November ; 4(11): 691–699. doi:10.1038/nchembio.117.

## Targeted polypharmacology: Discovery of dual inhibitors of tyrosine and phosphoinositide kinases

Beth Apse<sup>1</sup>, Jimmy A. Blair<sup>2</sup>, Beatriz Z. Gonzalez<sup>3,4</sup>, Tamim M. Nazif<sup>5</sup>, Morri E. Feldman<sup>1</sup>, Brian Aizenstein<sup>6</sup>, Randy Hoffman<sup>6</sup>, Roger L. Williams<sup>3</sup>, Kevan M. Shokat<sup>2,5</sup>, and Zachary A. Knight<sup>5,7</sup>

<sup>1</sup>Program in Chemistry and Chemical Biology, University of California, San Francisco

<sup>2</sup>Department of Chemistry, University of California, Berkeley, Berkeley, CA 94720

<sup>3</sup>MRC Laboratory of Molecular Biology, Hills Road, Cambridge CB2 2QH, UK

<sup>5</sup>Howard Hughes Medical Institute and Department of Cellular and Molecular Pharmacology, University of California, San Francisco

<sup>6</sup>Invitrogen Corporation, 501 Charmany Drive, Madison, WI 53719

### Abstract

The clinical success of multitargeted kinase inhibitors has stimulated efforts to identify promiscuous drugs with optimal selectivity profiles. It remains unclear to what extent such drugs can be rationally designed, particularly for combinations of targets that are structurally divergent. Here we report the systematic discovery of molecules that potently inhibit both tyrosine kinases and PI3-Ks, two protein families that are among the most intensely pursued cancer drug targets. Through iterative chemical synthesis, X-ray crystallography, and kinome-level biochemical profiling, we identify compounds that inhibit a spectrum of novel target combinations in these two families. Crystal structures reveal that the dual selectivity of these molecules is controlled by a hydrophobic pocket conserved in both enzyme classes and accessible through a rotatable bond in the drug skeleton. We show that one compound, PP121, blocks the proliferation of tumor cells by direct inhibition of oncogenic tyrosine kinases and PI3-Ks. These molecules demonstrate the feasibility of accessing a chemical space that intersects two families of oncogenes.

---

Users may view, print, copy, and download text and data-mine the content in such documents, for the purposes of academic research, subject always to the full Conditions of use:[http://www.nature.com/authors/editorial\\_policies/license.html#terms](http://www.nature.com/authors/editorial_policies/license.html#terms)

Correspondence: shokat@cmp.ucsf.edu.

<sup>4</sup>Present Address: Instituto de Química-Física “Rocasolano” (CSIC), Serrano 119, 28006 Madrid, Spain.

<sup>7</sup>Present Address: The Rockefeller University, 1230 York Ave., New York, NY 10021

**Author Contributions** B.A. and Z.A.K. synthesized the molecules, determined their IC<sub>50</sub> values, and performed cell proliferation assays. Z.A.K. performed the western blots. B.A. performed flow cytometry, angiogenesis, and imaging assays. B.G. and R.L.W. determined the PI3-K co-crystal structures. B.A. and J.A.B. determined the Src co-crystal structures. T.M.N. performed the HUVEC blots. B.A. and R.H. performed the SelectScreen. M.E.F. assisted with data analysis. Z.A.K. designed the experiments and wrote the paper, with input from B.A. and K.M.S.

**Competing Interest Statement** K.M.S., B.A., and Z.A.K. are joint inventors on UC Regents owned patent applications covering these molecules which have been licensed to Intellikine. K.M.S. and Z.A.K. hold stock and are consultants to Intellikine.

## INTRODUCTION

Tyrosine kinases promote cell growth, survival, and proliferation, and are the target of frequent oncogenic mutations in tumors<sup>1,2</sup>. Eight tyrosine kinase inhibitors have been approved for clinical use and dozens more are in late-stage development. As a critical part of their signaling function, most tyrosine kinases activate the lipid kinases of the phosphoinositide 3-kinase (PI3-K) family<sup>3</sup>. PI3-K family members include p110 $\alpha$ , which is the most frequently mutated kinase in human cancer<sup>4,5</sup>, and mTOR, which is a central regulator of cell growth<sup>3</sup>. In addition, the lipid phosphatase PTEN is a commonly inactivated tumor suppressor<sup>6</sup>. These observations have stimulated interest in the therapeutic potential of PI3-K inhibitors, and the first such molecules recently entered clinical trials<sup>7,8</sup>. Together, PI3-Ks and tyrosine kinases define an interconnected set of oncogenes that are the focus of intense drug discovery efforts.

We asked whether it would be possible to discover molecules that potently inhibit both tyrosine kinases and PI3-Ks. This was motivated by two lines of reasoning. First, reactivation of PI3-K signaling is a common mechanism of resistance to tyrosine kinase inhibitors<sup>9–12</sup>, and preclinical studies have shown efficacy by combining inhibitors of these two families<sup>13–16</sup>. For this reason, molecules that target both tyrosine kinases and PI3-Ks are likely to possess potent antitumor activity.

Second, we sought to identify chemical principles that might guide the discovery of molecules targeting these two families of oncogenes. While there are many examples of multitargeted kinase inhibitors, the targets of these drugs are not randomly distributed throughout the kinome<sup>2,17–19</sup>. Drugs that target certain combinations of kinases, but not others, tend to be repeatedly discovered. It would be desirable to instead rationally design promiscuous drugs based on the biological function of the targets, but it is unclear to what extent this can be achieved for proteins that are structurally divergent<sup>20</sup>.

Protein kinases and PI3-Ks diverged early in evolution<sup>21</sup> and therefore lack significant sequence similarity (Fig. 1). Nonetheless, these two enzyme families share several short motifs (e.g. the DFG sequence that coordinates Mg<sup>2+</sup>-ATP), and their kinase domains display a similar two-lobed architecture<sup>22</sup>. These enzymes also use a set of analogous residues to catalyze the phosphotransfer reaction, even though the orientation of key structural elements and the identity of most residues has diverged dramatically (Fig. 1).

Consistent with these structural differences, there is limited overlap among known inhibitors of protein kinases and PI3-Ks. A recent comprehensive profiling of kinase inhibitor selectivity tested 37 potent and structurally diverse protein kinase inhibitors against p110 $\alpha$  and found that none were active<sup>19</sup>; in the same study, the p110 $\alpha$  inhibitor PI-103 (**1**) showed little or no activity against over 300 protein kinases<sup>19</sup>. We have found that clinically approved protein kinase inhibitors bind to their primary target >10,000-fold more potently than any PI3-K (Supplementary Table 1 online). Nonetheless, pan-specific protein kinase inhibitors such as staurosporine (**2**) and quercetin (**3**) have been shown to inhibit PI3-Ks at micromolar concentrations<sup>23</sup>. In addition, there are at least two reports of high affinity interactions between a PI3-K inhibitor and a protein kinase: wortmannin (**4**) inhibits the

serine-threonine kinase PLK124, and an imidazoquinoline (**5**) inhibits the serine-threonine kinase PDK125. The structural basis for these interactions is not known.

We describe here the systematic discovery of small molecules that potently inhibit both tyrosine kinases and PI3-Ks. We trace the unique selectivity of these molecules to interactions within a hydrophobic pocket that is conserved between both enzyme classes. We demonstrate that one such molecule, PP121 (**6**), blocks the proliferation of tumor cells through direct inhibition of oncogenic tyrosine kinases and PI3-Ks, and further that this molecule evades a common mechanism of drug resistance by redundant inhibition of members of these two families.

## RESULTS

### Discovery of dual tyrosine kinase/PI3-K inhibitors

We screened a library of tyrosine kinase inhibitors for activity against the PI3-K p110 $\alpha$ . This screen yielded two pyrazolopyrimidines, S1 (**7**) and S2 (**8**), that inhibit several PI3-Ks at low micromolar concentrations (Fig. 2a and Supplementary Table 1 online). Structure-activity relationship (SAR) data revealed key elements of these hits required for PI3-K inhibition. For example, substitution of the exocyclic amine (N4) with *N*-methyl abolished activity against PI3-Ks, suggesting that this amino group may act as a hydrogen bond donor (Fig. 2a). At the R2 position, methyl and isopropyl but not *t*-butyl substituents were tolerated, placing steric constraint on substitution in that region.

The pyrazolopyrimidine is a well characterized nucleus for tyrosine kinase inhibition<sup>26–28</sup>, and we profiled S1 and S2 against over 200 protein kinases (Fig. 2b). These molecules displayed a selectivity pattern similar to the classical pyrazolopyrimidine kinase inhibitor PP1 (**9**; Fig. 2b), which inhibits Src family kinases, Abl, and several receptor tyrosine kinases (e.g. PDGFR and Ret) but is highly selective against the serine-threonine kinome.

Based on this data, we sought to optimize the potency and selectivity of S1 and S2. More than 200 analogs of these hits were iteratively synthesized through diversification of the R1 and R2 substituents (Supplementary Table 1 online). The progress of this chemistry was guided by testing each new compound against a panel of 14 tyrosine kinases and PI3-Ks, monitoring this extensive SAR in order to identify chemical features that favor binding to both target classes, and then incorporating these features into subsequent rounds of analogs (Supplementary Fig. 1 online).

From this effort we identified molecules that possess novel target profiles against kinases in both families (Fig. 2a). This included dual inhibitors such as PP121 and PP487 (**10**) that inhibit at nanomolar concentrations both PI3-Ks (e.g. p110 $\alpha$  and mTOR) and tyrosine kinases (e.g. Src, Abl, and the VEGF receptor). We profiled PP121 and PP487 against over 200 protein kinases and found that they inhibit a pattern of tyrosine kinases similar to clinically approved drugs such as dasatinib (**11**) and sunitinib (**12**), yet retain a high degree of selectivity against the serine-threonine kinome (Fig. 2b). Thus, these molecules are able to potently inhibit both tyrosine kinases and PI3-Ks without indiscriminately targeting all kinases.

## A selective mTOR inhibitor and other novel target profiles

Although our goal was to identify molecules that inhibit both tyrosine kinases and PI3-Ks, we discovered compounds with diverse and unexpected selectivity profiles (Fig. 2a). One such molecule was PP242 (**13**), which potently inhibited mTOR ( $IC_{50} = 8$  nM) but was much less active against other PI3-K family members (Fig. 2a). Testing of this compound against 219 protein kinases revealed remarkable selectivity relative to the protein kinase: at a concentration 100-fold above its  $IC_{50}$  for mTOR, PP242 inhibited only one kinase by more than 90% (Ret) and only three by more than 75% (PKC $\alpha$ , PKC $\beta$ II and JAK2 V617F; Fig. 2b and Supplementary Table 2 online). mTOR has emerged as an important drug target, and PP242 is the first selective and ATP competitive inhibitor of mTOR that has been described. Unlike rapamycin, PP242 targets both mTOR complexes and therefore can be used to explore signaling by mTORC2. We treated BT549 cells with PP242 and found that this molecule inhibited the phosphorylation of Akt, the mTOR substrate p70S6K, and its downstream target S6 (Supplementary Fig. 2 online). These data are consistent with a requirement for mTOR kinase activity in Akt phosphorylation<sup>29</sup>, and we have used PP242 to dissect mTOR signaling (manuscript submitted).

We were surprised by the diversity of target profiles that could be achieved by structural variation within the pyrazolopyrimidine chemotype (Fig. 2a). In many cases, small changes in structure produced dramatic alterations in selectivity. For example, the DNA-PK selective inhibitor PP162 (**14**) and the multitargeted dual inhibitor PP121 differ only in the arrangement of nitrogen atoms in the R1 ring (Fig. 2a). Conversely, the highly selective p110 $\delta$  inhibitor PIK-294 (**15**) contains the pyrazolopyrimidine core embedded within a structure derived from an unrelated chemical series<sup>18</sup> (Fig. 2a). When PIK-294 is compared to tyrosine kinase selective pyrazolopyrimidines such as PP20 (**16**), these two molecules span more than  $10^8$ -fold in relative target selectivity (Fig. 2a).

To obtain a global view of the target selectivity of these molecules, we compared 172 pyrazolopyrimidines based on their  $IC_{50}$  values against 13 tyrosine kinases and PI3-Ks using principal component analysis (PCA) (Fig. 2c). The proximity of compounds in this two-dimensional space provides a visual representation of their similarity against the 13 kinase targets, and we included as reference compounds four clinically approved tyrosine kinase inhibitors (sorafenib (**17**), gefitinib (**18**), dasatinib, and sunitinib) and four widely-used PI3-K inhibitors (wortmannin, PI-103, IC87114 (**19**), and PIK-90 (**20**)). This analysis revealed that most pyrazolopyrimidines occupy a region of selectivity space intermediate between selective PI3-K and tyrosine kinase inhibitors (Fig. 2c), consistent with the targeted profile of these compounds. By contrast, pyrazolopyrimidines such as PP20 and PIK294 that preferentially inhibit either PI3-Ks or tyrosine kinases co-localized with reference compounds that are selective for either family (Fig. 2c). This provides an unbiased representation of the target profiles of these various classes of inhibitors.

## Structure of pyrazolopyrimidines bound to p110 $\gamma$

We determined crystal structures of S1 and S2 bound to p110 $\gamma$  in order to understand how this chemotype binds to PI3-Ks (Fig. 3). In these structures, the pyrazolopyrimidine N4 and N5 nitrogens make hydrogen bonds to the kinase hinge residues Glu880 and Val882,

respectively (Fig. 3). Similar hydrogen bonds are made by adenine in ATP bound structures<sup>22</sup>, and these interactions account for SAR suggesting that the exocyclic amine at N4 is a hydrogen bond donor to PI3-Ks.

The R1 aryl substituents of S1 and S2 project into a deeper pocket in p110 $\gamma$  that extends beyond the region occupied by ATP. In this region, the *m*-phenol of S1 makes a hydrogen bond to the catalytic lysine (Lys833 in p110 $\gamma$ ), whereas the 2-naphthyl of S2 makes extensive hydrophobic interactions (Fig. 3). We have previously shown that chemically diverse PI3-K inhibitors make interactions in this pocket that are required for high affinity binding<sup>18</sup>.

### A gatekeeper for protein kinases but not PI3-Ks

We sought to understand how molecules such as PP121 can potently inhibit both tyrosine kinases and PI3-Ks but not serine-threonine kinases. Tyrosine and serine-threonine kinases are closely related to each other but only distantly related to the PI3-K family<sup>21</sup>. For this reason, it was surprising that we were able to broaden the selectivity of pyrazolopyrimidines to target PI3-Ks without introducing activity against the more numerous serine-threonine kinases. To account for this, we searched for structural features that are conserved between PI3-Ks and tyrosine kinases and may be utilized by these molecules to achieve their selectivity.

Within the protein kinase family, the selectivity of pyrazolopyrimidines is controlled by the size of a single amino acid, termed the gatekeeper<sup>27,28</sup>. Most tyrosine kinases possess a small residue (threonine or valine) at this position and are more sensitive to these drugs, whereas most serine-threonine kinases possess a larger residue (such as isoleucine or methionine) and are less sensitive. We tested the compounds in our panel against a T338I gatekeeper mutant of the tyrosine kinase Src and found that this mutation was sufficient to confer broad inhibitor resistance (Fig. 4a). Thus, the size of the gatekeeper residue controls the protein kinase selectivity of these drugs by preventing binding to most serine-threonine kinases.

PI3-Ks possess an isoleucine at the position that is structurally analogous to the gatekeeper within the PI3-K family (Fig. 1b). For this reason, the potent inhibition of PI3-Ks by the pyrazolopyrimidine chemotype was surprising. We determined crystal structures of four compounds bound to c-Src (S1, PP121, PP102 (**21**), PP494 (**22**)) and compared these to the structures of S1 and S2 bound to p110 $\gamma$ . Because c-Src and p110 $\gamma$  differ in many aspects of their structure (Fig. 1a), we focused first on analyzing only the relative orientation of the gatekeeper residue, the adenine of ATP, and the drug within the active site of each kinase.

In the Src structures, the pyrazolopyrimidine superimposes with the adenine of ATP, positioning the R1 aryl substituent of the drug to project past the gatekeeper (Thr338) into the hydrophobic pocket (Fig. 4b,c). This is consistent with previously reported structures of pyrazolopyrimidines bound to tyrosine kinases<sup>28</sup>. When we compared this to the PI3-K structures, we noticed that the residue analogous to the gatekeeper in PI3-Ks (Ile879) is shifted both vertically and horizontally relative to its counterpart in protein kinases (Fig. 4c). This structural difference is accompanied by an alteration of the drug binding mode: the

pyrazolopyrimidine core is displaced from alignment with ATP and the R1 aryl substituent is rotated 90° (Fig. 4b). The combined effect of these structural differences and compound movements is that, in the PI3-K structures, the R1 substituent of the drug projects underneath, rather than adjacent to, the side-chain of the gatekeeper (Fig. 4c). This enables these molecules to make interactions with the deeper hydrophobic pocket in PI3-Ks despite the presence of a sterically demanding isoleucine at the gatekeeper position. This provides a structural rationale for the inhibition of PI3-Ks, but not serine-threonine kinases, by the pyrazolopyrimidine chemotype.

### Potent dual inhibitors target conserved catalytic residues

We synthesized many pyrazolopyrimidines, but only a few, such as PP121 and PP487, potently inhibit both tyrosine kinases and PI3-Ks. We analyzed the co-crystal structures of these and related compounds in order to identify interactions that may contribute to their unique dual potency.

All protein kinases contain a conserved glutamic acid (Glu310 in Src) that makes a hydrogen bond to the catalytic lysine (Lys295 in Src). This interaction organizes the active site for catalysis and stabilizes helix C in an active conformation (Fig. 4d, top panel). The importance of these residues is underscored their functional conservation across diverse kinases that share no sequence homology with the protein kinase superfamily<sup>21</sup>. Structures of pyrazolopyrimidines bound to protein kinases reveal that these drugs disrupt the interaction between Glu310 and Lys295, resulting in helix C adopting a disordered or inactive conformation (Fig. 4d, center panel). However, in the crystal structure of PP121 bound to Src, this molecule makes a hydrogen bond to Glu310, effectively substituting for the structural role of the catalytic lysine (Fig. 4d, bottom panel). This interaction has a dramatic effect on the structure of the kinase, resulting in the ordering of helix C and stabilization of an active conformation (Fig. 4d and Supplementary Movie). It is likely that this interaction contributes to the more potent inhibition of tyrosine kinases by PP121 relative to closely related molecules such as PP102, which cannot make the same hydrogen bond.

We have not obtained a crystal structure of PP121 bound to p110 $\gamma$ , but a structurally analogous hydrogen bond is possible in PI3-Ks (Supplementary Fig. 3 online). This suggests that PP121 achieves its dual potency by targeting a residue (Glu310 in Src) that has been structurally conserved between kinase families. Interestingly, the compound S1 makes a hydrogen bond to two residues that are also highly conserved in each kinase family: the catalytic lysine in PI3-Ks and the gatekeeper threonine in tyrosine kinases.

Based on these data, we propose that molecules such as PP121 achieve their dual selectivity by combining two molecular recognition steps. First, the size of the gatekeeper acts as a filter to block binding of pyrazolopyrimidines to most serine-threonine kinases. This filter does not block binding to PI3-Ks, because the gatekeeper is in a different orientation in this kinase family. Second, the most potent dual inhibitors make specific hydrogen bonds to a small subset of residues, such as Lys295 and Glu310 in Src, that are conserved between protein and lipid kinases and neighbor the gatekeeper pocket.

## PP121 inhibits PI3-Ks and mTOR in tumor cells

We next explored the cellular effects of the dual inhibitor PP121. Our goal was to dissect the activity of this compound into distinct components resulting from direct inhibition of individual PI3-Ks (e.g. p110 $\alpha$  and mTOR) or tyrosine kinases (e.g. Src, Abl, Ret, and the VEGF receptor). To do this, we systematically compared PP121 to six reference compounds (Fig. 5a). This panel includes three PI3-K inhibitors (PIK-90, PI7-103, and PP102) and three tyrosine kinase inhibitors (PP1, sorafenib, and imatinib (**23**)) that each inhibit different subsets of kinases within these two families.

We first measured the effect of these drugs on signaling through the PI3-K, mTOR, and MAPK pathways in two glioblastoma cell lines, U87 and LN229 (Fig. 4a–c). PP121 and PP102 potently and dose-dependently blocked the phosphorylation of Akt, p70S6K and S6 in these cells (Fig. 5b,c). This inhibition was more potent in LN229 cells, which, unlike U87 cells, express functional PTEN30 (Fig. 5b,c). We have observed a similar dose shift for the PI3-K inhibitors PIK-90 and PI-103 in these two cell lines31.

In contrast to their potent blockade of PI3-K/mTOR signaling, PP121 and PP102 had no effect on the phosphorylation of Erk at concentrations up to 10  $\mu$ M (Fig. 5b,c). This suggests that PP121 and PP102 block the PI3-K pathway by direct inhibition of PI3-K/mTOR in these cells, rather than through inhibition of an upstream tyrosine kinase. This conclusion is supported by the fact that the tyrosine kinase inhibitor sorafenib, which shares several targets with PP121 (e.g. PDGFR, Ret, and VEGFR2), had no effect on PI3-K/mTOR signaling in these cells (Fig. 5b,c).

We next tested the ability of PP121 to block proliferation of a diverse panel of tumor cell lines containing mutations in the PI3-K pathway components *PIK3CA*, *PTEN*, or *RAS*. Each cell line was assayed at three serum concentrations to explore the possibility that the requirement for PI3-K signaling is magnified under conditions of growth factor deprivation32.

PP121 potently inhibited the proliferation of a subset of these lines, and the pattern of its antiproliferative activity was remarkably similar to the PI3-K/mTOR inhibitor PI-103 (Fig. 5d, top panel). The parallel activity of these two structurally unrelated molecules strongly suggests that they block cell proliferation through inhibition of a common target. By contrast, the tyrosine kinase inhibitor sorafenib was largely inactive (Fig. 5d).

We performed cell cycle analysis by flow cytometry to determine the nature of the proliferative block caused by these drugs. PP121 induced a G<sub>0</sub>G<sub>1</sub> arrest in most tumor cells (Fig. 5e). This arrest was similar to the effect of treatment with PI-103 (Fig. 5e) and is characteristic of combined inhibition of PI3-K and mTOR in these cells31. Together, these data demonstrate that PP121 blocks the proliferation of tumor cell lines containing PI3-K pathway mutations by direct inhibition of PI3-Ks and mTOR.

Direct inhibition of mTOR is likely to be particularly important for the antiproliferative activity of PP121. The PI3-K inhibitors PP102 and PIK-90, which are less active against mTOR, also displayed less antiproliferative activity in these cells (Fig. 5d, bottom). In



addition, we have shown previously that direct mTOR inhibition is required for robust blockade of cell proliferation by diverse PI3-K family inhibitors<sup>16,31</sup>. Nonetheless, the molecular basis for this difference remains enigmatic, since PI3-K inhibitors such as PP102 and PIK-90 potentially block the phosphorylation of mTOR substrates (e.g. Akt and p70S6K) indirectly via upstream PI3-K inhibition<sup>31</sup> (Fig. 5b,c). In this respect, it is noteworthy that two of the first PI3-K inhibitors to enter clinical trials, NVP-BEZ235 (**24**) and XL765 (**25**), are also potent and direct mTOR inhibitors<sup>33</sup>.

### PP121 inhibits oncogenic Src and Ret

PP121 inhibits several tyrosine kinases that are prominent cancer drug targets, including Bcr-Abl, Src, Ret, and the VEGF receptor (Fig. 2a). We therefore explored the activity of PP121 in cells that express these tyrosine kinases, in order to understand how this activity cooperates with inhibition of PI3-Ks and mTOR.

Transformation of fibroblasts by the viral oncogene v-Src results in dysregulated tyrosine phosphorylation and cytoskeletal rearrangements. As PP121 potently inhibits Src *in vitro* ( $IC_{50} = 14$  nM; Fig. 2a), we tested the ability of PP121 to reverse v-Src mediated cellular transformation. PP121 blocked tyrosine phosphorylation induced by v-Src and restored actin stress fiber staining, and the magnitude of these effects was similar to treatment with the Src family kinase inhibitor PP1 (Fig. 6). By contrast, PI-103 inhibited signaling through the PI3-K/mTOR pathway but had no effect on either phosphotyrosine levels or cell morphology (Fig. 6). Thus, PP121 directly inhibits Src in cells and reverses its biochemical and morphological effects.

Oncogenic mutations in the Ret receptor tyrosine kinase are frequently found in thyroid tumors<sup>34</sup> and PP121 potently inhibits the Ret kinase domain *in vitro* ( $IC_{50} < 1$  nM). We therefore explored the activity of this compound in TT thyroid carcinoma cells that express the C634W oncogenic Ret mutant<sup>35</sup>. PP121 inhibited Ret autophosphorylation in cells at low nanomolar concentrations (Fig. 7a). This was similar to the effect of sorafenib (Fig. 7a), which is currently in clinical testing for thyroid cancer based in part on its activity against Ret kinase<sup>34,36</sup>. In contrast, the PI3-K/mTOR inhibitor PI-103 blocked the phosphorylation of S6 but had no effect on Ret autophosphorylation (Fig. 7a).

We compared the ability of these compounds to block the proliferation of TT thyroid carcinoma cells (Fig. 7b). PP121 inhibited proliferation of these cells at low nanomolar concentrations ( $IC_{50} = 50$  nM), whereas the Ret inhibitor sorafenib ( $IC_{50} = 780$  nM) and PI3-K/mTOR inhibitor PI-103 ( $IC_{50} \approx 800$  nM) were significantly less potent (Fig. 7b). The PI3-K inhibitors PIK-90 ( $IC_{50} = 1.4$   $\mu$ M) and PP102 ( $IC_{50} = 2.2$   $\mu$ M) were active only at micromolar concentrations (Fig. 7b). The unique ability of PP121 to simultaneously inhibit Ret, PI3-Ks, and mTOR likely contributes to its exceptional potency in this setting.

### PP121 directly inhibits the VEGF receptor

The VEGF receptor (VEGFR2) is a key target of two clinically approved small molecule drugs (sunitinib and sorafenib) and PI3-K/mTOR signaling is critical for VEGF mediated angiogenesis<sup>37,38</sup>. As PP121 potently inhibits the VEGFR2 kinase domain *in vitro* ( $IC_{50} =$

12 nM; Fig. 2a), we tested the ability of PP121 to block VEGF signaling in human umbilical vein endothelial cells (HUVECs) that endogenously express VEGFR2. PP121 potently blocked VEGF stimulated activation of the PI3-K and MAPK pathways (Supplementary Fig. 4 online). In addition, PP121 inhibited VEGFR2 autophosphorylation at low nanomolar concentrations, confirming that this molecule directly targets VEGFR2 in cells.

We compared the effects of PP121 with the closely related pyrazolopyrimidine PP102. This compound is less potent than PP121 against VEGFR2 *in vitro* but has similar activity against PI3-Ks (Fig. 2a). Consistent with this selectivity profile, PP102 inhibited the phosphorylation of Akt and S6 in cells at low nanomolar concentrations but was much less potent at blocking the phosphorylation of VEGFR2 and Erk (Supplementary Fig. 4 online). We measured the effect of these compounds on the proliferation of endothelial cells stimulated with either complete media or VEGF alone. PP121 and PP102 both inhibited HUVEC proliferation in complete media at micromolar concentrations, but PP121 displayed a selective enhancement in potency against cells stimulated only with VEGF ( $IC_{50} = 41$  nM; Supplementary Fig. 4 online). These data are consistent with more robust inhibition of VEGF signaling by PP121 relative to analogs such as PP102 that do not potently target VEGFR2.

Angiogenesis is multistep process involving endothelial cell proliferation, migration, and extracellular matrix (ECM) remodelling. We therefore tested these compounds in a functional angiogenesis assay that measures the ability of HUVECs to form three-dimensional tubes within a tumor-derived ECM. PP121 potently blocked tube formation in this assay ( $IC_{50} = 0.31$  nM) whereas PI-103 and sorafenib were somewhat less active ( $IC_{50} = 0.60$  and  $0.59$  nM, respectively). The selective PI3-K inhibitors PIK-90 and PP102 inhibited tube formation only at micromolar concentrations (Supplementary Fig. 4 online). This spectrum of activities is consistent with multi-level collaboration between tyrosine kinases, PI3-Ks, and mTOR in angiogenic signaling.

### PP121 overrides resistance in CML by redundant targeting

Chronic myelogenous leukemia (CML) is caused by a chromosomal translocation that generates the Bcr-Abl oncogene<sup>39</sup>. Three clinically approved drugs target this tyrosine kinase, and each of these drugs is sensitive to an overlapping but distinct set of Bcr-Abl resistance mutations<sup>40,41</sup>. PP121 inhibits the Abl kinase *in vitro* ( $IC_{50} = 18$  nM; Fig. 2b), and PI3-K/mTOR signaling cooperates with Bcr-Abl to drive CML cell proliferation<sup>15</sup>. We therefore measured the activity of PP121 in cellular models of normal and drug-resistant CML in order to investigate the interplay between Bcr-Abl, PI3-K, and mTOR in this setting.

PP121 inhibited Bcr-Abl induced tyrosine phosphorylation in K562 cells as well as BaF3 cells that express Bcr-Abl, and the potency of PP121 was similar to the clinically approved drug imatinib (Fig. 8a and Supplementary Fig. 5 online). Consistent with this biochemical activity, PP121 robustly blocked the proliferation of both cell lines (Fig. 8b and Supplementary Fig. 5 online). This was the result of drug-induced apoptosis in K562 cells and a combination of apoptosis and cell cycle arrest in Bcr-Abl expressing BaF3 cells (Fig. 8c,d).

In contrast to PP121, PI-103 did not block Bcr-Abl mediated tyrosine phosphorylation but did inhibit signaling through the mTOR pathway (Fig. 8a). Correspondingly, PI-103 induced cell cycle arrest but not apoptosis (Fig. 8c,d). The PI3-K inhibitors PIK-90 and PP102 had little effect on cell proliferation (Fig. 8b), consistent with their activity in other settings. Together, these data demonstrate that PP121, but not other PI3-K or mTOR inhibitors, directly inhibits Bcr-Abl and thereby kills CML cells.

Clinical resistance to Bcr-Abl inhibitor therapy is caused by mutations in the kinase that prevent drug binding<sup>40,41</sup>. The most common resistance mutation is Bcr-Abl T315I, which increases the size of the gatekeeper residue from threonine to isoleucine. This mutation blocks the binding of all clinically approved kinase inhibitors and also confers resistance to inhibition by PP121 ( $IC_{50} > 1 \mu M$ ; Supplementary Table 2 online). We tested PP121 in BaF3 cells that express Bcr-Abl T315I and found that this mutation abrogated the ability of PP121 to inhibit cellular tyrosine phosphorylation (Fig. 8a) and induce apoptosis (Fig. 8c). This confirms that the cytotoxicity of PP121 in CML cells is a consequence of direct Bcr-Abl inhibition; we obtained similar results with imatinib (Fig. 8a,c).

Unlike imatinib, however, PP121 retained the ability to potently block the proliferation of Bcr-Abl T315I expressing cells (Fig. 8b). This proliferative block was due to a  $G_0G_1$  cell cycle arrest that was similar to the effect of PI-103 treatment (Fig. 8d). Consistent with this arrest, PP121 potently inhibited the phosphorylation of S6 even in cells expressing Bcr-Abl T315I (Fig. 8a). We attribute this residual inhibition of S6 phosphorylation to direct inhibition of PI3-K/mTOR by PP121 that is unaffected by Bcr-Abl mutation. Thus, PP121 is able to evade drug resistance caused by mutation of a single kinase by redundantly targeting two pathways: Bcr-Abl mediated cell survival and PI3-K/mTOR mediated cell proliferation. This mechanism of action is complementary to ongoing efforts to identify inhibitors that target specific Bcr-Abl mutant alleles<sup>42</sup>.

## DISCUSSION

Effective therapy for many cancers will require the simultaneous inhibition of multiple oncogenic kinases<sup>9,10,31,42,43</sup>. This is because tumor cells rapidly develop resistance to inhibitors of individual kinases, either through mutation of the target to prevent drug binding<sup>40,41</sup>, activation of surrogate kinases to substitute for the drug target<sup>9</sup>, or modulation of pathway components to buffer against incomplete inhibition<sup>10</sup>. Even in the absence of acquired resistance, there are few examples of selective kinase inhibitors that have substantial anti-tumor activity as monotherapy, indicating that inhibition of additional targets will be required<sup>1,43</sup>.

Multitargeted drugs will be an important tool in meeting this challenge<sup>44–46</sup>, but it is unclear to what extent the selectivity of these molecules can be rationally designed, particularly for combinations of targets that are structurally divergent<sup>2,20</sup>. Progress toward this goal will require the discovery of chemical and structural features that link important classes of drug targets, and the use of these features to guide the design of promiscuous drugs with customized selectivity profiles. The chemical principles that will enable this type of targeted polypharmacology remain largely unknown, but the successful pursuit of single-

targeted kinase inhibitors provides reason for optimism. In that setting, the early identification of key selectivity determinants, such as the inactive conformation<sup>44,45</sup>, allosteric sites<sup>46</sup>, reactive cysteine residues<sup>47,48</sup>, and the gatekeeper<sup>27,28</sup>, has now led to the systematic design of molecules that target these features.

We asked whether it would be possible to discover molecules that target both tyrosine kinases and PI3-Ks. These two protein families are among the most intensely pursued cancer drug targets, but they are significantly more divergent than the typical targets of multitargeted drugs. We show here that it is possible to identify potent, selective, and drug-like molecules that target these two families of oncogenic kinases, and we further elucidate the structural features that control the unique selectivity of these molecules. This expands the landscape of target selectivities that are accessible to rational drug design. As several clinically approved kinase inhibitors are believed to act through serendipitous target combinations, exploration of such chemical space may be a productive strategy for discovering molecules with emergent properties.

## METHODS

### Chemical Synthesis

All compounds were synthesized from commercially available starting materials and purified by RP-HPLC. See Supplementary Methods online for complete details.

### *In vitro* kinase assays

Purified kinase domains were incubated with inhibitors at 2- or 4-fold dilutions over a concentration range of 50 - 0.001  $\mu$ M or with vehicle (0.1% DMSO) in the presence of 10  $\mu$ M ATP, 2.5  $\mu$ Ci of  $\gamma$ -<sup>32</sup>P-ATP and substrate. Reactions were terminated by spotting onto nitrocellulose or phosphocellulose membranes, depending on the substrate; this membrane was then washed 5–6 times to remove unbound radioactivity and dried. Transferred radioactivity was quantitated by phosphorimaging and IC<sub>50</sub> values were calculated by fitting the data to a sigmoidal doseresponse using Prism software.

### X-ray crystallography

p110 $\gamma$  and Src were recombinantly expressed, purified, and crystallized in the presence of inhibitors by hanging-drop vapor diffusion. Structures were solved from diffraction data by molecular replacement. See Supplementary Methods online for additional details.

### Cell culture and western blot analysis

Cells were grown in 12-well plates and treated with inhibitor at the indicated concentrations or vehicle (0.1% DMSO). Treated cells were lysed, lysates were resolved by SDS-PAGE, transferred to nitrocellulose and blotted. All antibodies were purchased from Cell Signalling Technology.

### Cell proliferation assays

Cells grown in 96-well plates were treated with inhibitor at 4-fold dilutions (10  $\mu$ M - 0.040  $\mu$ M) or vehicle (0.1% DMSO). After 72 h cells were exposed to Resazurin sodium salt (22

$\mu\text{M}$ , Sigma) and fluorescence was quantified.  $\text{IC}_{50}$  values were calculated using Prism software. For proliferation assays involving single cell counting, non-adherent cells were plated at low density (3–5% confluence) and treated with drug (2.5  $\mu\text{M}$ ) or vehicle (0.1% DMSO). Cells were diluted into trypan blue daily and viable cells counted using a hemocytometer.

### Apoptosis and cell cycle analysis

Cells were treated with the indicated concentration of inhibitor or vehicle (0.1% DMSO) for 24–72 h. Cells were either stained live with AnnexinV-FITC or fixed with ethanol and stained with propidium iodide. Cell populations were separated using a FACS Calibur flow cytometer; data was collected using CellQuest Pro software and analyzed with either ModFit or FlowJo Software.

### Supplementary Material

Refer to Web version on PubMed Central for supplementary material.

### Acknowledgements

We thank W. Weiss for providing glioblastoma cells, M. Korn for providing Seg1 cells, N. Shah for providing BaF3 Bcr-Abl and BaF3 Bcr-Abl T3151 cells, and D. Hanahan for  $\beta\text{TC3}$  cells. We thank P.J. Alaimo for synthetic intermediates that were used to prepare several compounds, and J.L. Garrison for helpful comments on the text. This work was supported by the Sandler Program in Asthma Research and NIH grant AI44009.

### REFERENCES

1. Krause DS, Van Etten RA. Tyrosine kinases as targets for cancer therapy. *N Engl J Med.* 2005; 353:172–187. [PubMed: 16014887]
2. Sebolt-Leopold JS, English JM. Mechanisms of drug inhibition of signalling molecules. *Nature.* 2006; 441:457–462. [PubMed: 16724058]
3. Shaw RJ, Cantley LC. Ras, PI(3)K and mTOR signalling controls tumour cell growth. *Nature.* 2006; 441:424–430. [PubMed: 16724053]
4. Samuels Y, et al. High frequency of mutations of the PIK3CA gene in human cancers. *Science.* 2004; 304:554. [PubMed: 15016963]
5. Samuels Y, Velculescu VE. Oncogenic mutations of PIK3CA in human cancers. *Cell Cycle.* 2004; 3:1221–1224. [PubMed: 15467468]
6. Li J, et al. PTEN, a putative protein tyrosine phosphatase gene mutated in human brain, breast, and prostate cancer. *Science.* 1997; 275:1943–1947. [PubMed: 9072974]
7. Knight ZA, Shokat KM. Chemically targeting the PI3K family. *Biochem Soc Trans.* 2007; 35:245–249. [PubMed: 17371250]
8. Maira SM, et al. Identification and characterization of NVP-BEZ235, a new orally available dual phosphatidylinositol 3-kinase/mammalian target of rapamycin inhibitor with potent in vivo antitumor activity. *Mol Cancer Ther.* 2008
9. Engelman JA, et al. MET amplification leads to gefitinib resistance in lung cancer by activating ERBB3 signaling. *Science.* 2007; 316:1039–1043. [PubMed: 17463250]
10. Sergina NV, et al. Escape from HER-family tyrosine kinase inhibitor therapy by the kinase-inactive HER3. *Nature.* 2007; 445:437–441. [PubMed: 17206155]
11. Haas-Kogan DA, et al. Epidermal growth factor receptor, protein kinase B/Akt, and glioma response to erlotinib. *J Natl Cancer Inst.* 2005; 97:880–887. [PubMed: 15956649]
12. Mellingerhoff IK, et al. Molecular determinants of the response of glioblastomas to EGFR kinase inhibitors. *N Engl J Med.* 2005; 353:2012–2024. [PubMed: 16282176]

13. Fan QW, et al. Combinatorial efficacy achieved through two-point blockade within a signaling pathway—a chemical genetic approach. *Cancer Res.* 2003; 63:8930–8938. [PubMed: 14695210]
14. Wang MY, et al. Mammalian target of rapamycin inhibition promotes response to epidermal growth factor receptor kinase inhibitors in PTEN-deficient and PTEN-intact glioblastoma cells. *Cancer Res.* 2006; 66:7864–7869. [PubMed: 16912159]
15. Mohi MG, et al. Combination of rapamycin and protein tyrosine kinase (PTK) inhibitors for the treatment of leukemias caused by oncogenic PTKs. *Proc Natl Acad Sci U S A.* 2004; 101:3130–3135. [PubMed: 14976243]
16. Fan QW, et al. A dual phosphoinositide-3-kinase alpha/mTOR inhibitor cooperates with blockade of epidermal growth factor receptor in PTEN-mutant glioma. *Cancer Res.* 2007; 67:7960–7965. [PubMed: 17804702]
17. Knight ZA, Shokat KM. Features of selective kinase inhibitors. *Chem Biol.* 2005; 12:621–637. [PubMed: 15975507]
18. Knight ZA, et al. A pharmacological map of the PI3-K family defines a role for p110alpha in insulin signaling. *Cell.* 2006; 125:733–747. [PubMed: 16647110]
19. Karaman MW, et al. A quantitative analysis of kinase inhibitor selectivity. *Nat Biotechnol.* 2008; 26:127–132. [PubMed: 18183025]
20. Hopkins AL, Mason JS, Overington JP. Can we rationally design promiscuous drugs? *Curr Opin Struct Biol.* 2006; 16:127–136. [PubMed: 16442279]
21. Scheeff ED, Bourne PE. Structural evolution of the protein kinase-like superfamily. *PLoS Comput Biol.* 2005; 1:e49. [PubMed: 16244704]
22. Walker EH, Perisic O, Ried C, Stephens L, Williams RL. Structural insights into phosphoinositide 3-kinase catalysis and signalling. *Nature.* 1999; 402:313–320. [PubMed: 10580505]
23. Walker EH, et al. Structural determinants of phosphoinositide 3-kinase inhibition by wortmannin, LY294002, quercetin, myricetin, and staurosporine. *Mol Cell.* 2000; 6:909–919. [PubMed: 11090628]
24. Liu Y, et al. Wortmannin, a widely used phosphoinositide 3-kinase inhibitor, also potently inhibits mammalian polo-like kinase. *Chem Biol.* 2005; 12:99–107. [PubMed: 15664519]
25. Stauffer F, Maira SM, Furet P, Garcia-Echeverria C. Imidazo[4,5-c]quinolines as inhibitors of the PI3K/PKB-pathway. *Bioorg Med Chem Lett.* 2008; 18:1027–1030. [PubMed: 18248814]
26. Hanke JH, et al. Discovery of a novel, potent, and Src family-selective tyrosine kinase inhibitor. Study of Lck- and FynT-dependent T cell activation. *J Biol Chem.* 1996; 271:695–701. [PubMed: 8557675]
27. Liu Y, et al. Structural basis for selective inhibition of Src family kinases by PP1. *Chem Biol.* 1999; 6:671–678. [PubMed: 10467133]
28. Schindler T, et al. Crystal structure of Hck in complex with a Src family-selective tyrosine kinase inhibitor. *Mol Cell.* 1999; 3:639–648. [PubMed: 10360180]
29. Sarbassov DD, Guertin DA, Ali SM, Sabatini DM. Phosphorylation and regulation of Akt/PKB by the rictor-mTOR complex. *Science.* 2005; 307:1098–1101. [PubMed: 15718470]
30. Ishii N, et al. Frequent co-alterations of TP53, p16/CDKN2A, p14ARF, PTEN tumor suppressor genes in human glioma cell lines. *Brain Pathol.* 1999; 9:469–479. [PubMed: 10416987]
31. Fan QW, et al. A dual PI3 kinase/mTOR inhibitor reveals emergent efficacy in glioma. *Cancer Cell.* 2006; 9:341–349. [PubMed: 16697955]
32. Samuels Y, et al. Mutant PIK3CA promotes cell growth and invasion of human cancer cells. *Cancer Cell.* 2005; 7:561–573. [PubMed: 15950905]
33. Maira SM, et al. Identification and characterization of NVP-BEZ235, a new orally available dual phosphatidylinositol 3-kinase/mammalian target of rapamycin inhibitor with potent in vivo antitumor activity. *Mol Cancer Ther.* 2008; 7:1851–1863. [PubMed: 18606717]
34. Carlomagno F, et al. BAY 43-9006 inhibition of oncogenic RET mutants. *J Natl Cancer Inst.* 2006; 98:326–334. [PubMed: 16507829]
35. Carlomagno F, et al. Point mutation of the RET proto-oncogene in the TT human medullary thyroid carcinoma cell line. *Biochem Biophys Res Commun.* 1995; 207:1022–1028. [PubMed: 7864888]

36. Gupta-Abramson V, et al. Phase II Trial of Sorafenib in Advanced Thyroid Cancer. *J Clin Oncol*. 2008
37. Graupera M, et al. Angiogenesis selectively requires the p110alpha isoform of PI3K to control endothelial cell migration. *Nature*. 2008; 453:662–666. [PubMed: 18449193]
38. Guba M, et al. Rapamycin inhibits primary and metastatic tumor growth by antiangiogenesis: involvement of vascular endothelial growth factor. *Nat Med*. 2002; 8:128–135. [PubMed: 11821896]
39. de Klein A, et al. A cellular oncogene is translocated to the Philadelphia chromosome in chronic myelocytic leukaemia. *Nature*. 1982; 300:765–767. [PubMed: 6960256]
40. Shah NP, et al. Multiple BCR-ABL kinase domain mutations confer polyclonal resistance to the tyrosine kinase inhibitor imatinib (STI571) in chronic phase and blast crisis chronic myeloid leukemia. *Cancer Cell*. 2002; 2:117–125. [PubMed: 12204532]
41. Gorre ME, et al. Clinical resistance to STI-571 cancer therapy caused by BCR-ABL gene mutation or amplification. *Science*. 2001; 293:876–880. [PubMed: 11423618]
42. Sawyers CL. Cancer: mixing cocktails. *Nature*. 2007; 449:993–996. [PubMed: 17960228]
43. Stommel JM, et al. Coactivation of receptor tyrosine kinases affects the response of tumor cells to targeted therapies. *Science*. 2007; 318:287–290. [PubMed: 17872411]
44. Schindler T, et al. Structural mechanism for STI-571 inhibition of abelson tyrosine kinase. *Science*. 2000; 289:1938–1942. [PubMed: 10988075]
45. Liu Y, Gray NS. Rational design of inhibitors that bind to inactive kinase conformations. *Nat Chem Biol*. 2006; 2:358–364. [PubMed: 16783341]
46. Dudley DT, Pang L, Decker SJ, Bridges AJ, Saltiel AR. A synthetic inhibitor of the mitogen-activated protein kinase cascade. *Proc Natl Acad Sci U S A*. 1995; 92:7686–7689. [PubMed: 7644477]
47. Fry DW, et al. Specific, irreversible inactivation of the epidermal growth factor receptor and erbB2, by a new class of tyrosine kinase inhibitor. *Proc Natl Acad Sci U S A*. 1998; 95:12022–12027. [PubMed: 9751783]
48. Cohen MS, Zhang C, Shokat KM, Taunton J. Structural bioinformatics-based design of selective, irreversible kinase inhibitors. *Science*. 2005; 308:1318–1321. [PubMed: 15919995]

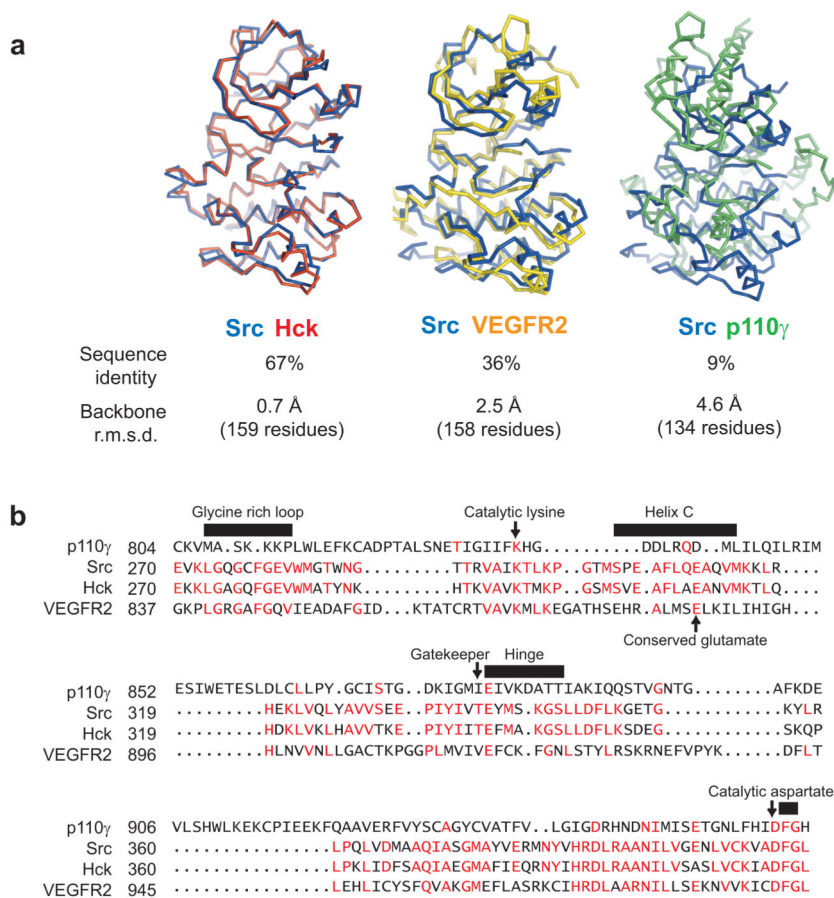


**Figure 1. Structural and sequence comparison of tyrosine kinases and PI3-Ks**  
**(a)** Backbone traces of crystal structures of the kinase domain of c-Src aligned to the kinase domain of the Src-family tyrosine kinase Hck (left), the receptor tyrosine kinase VEGFR2 (center) and the PI3-K p110 $\gamma$  (right). Statistics for the pairwise sequence identity and backbone r.m.s.d. are shown below. The number of residues used for each alignment is shown in parentheses. **(b)** Sequence alignment of the kinase domains of the tyrosine kinases c-Src, Hck, and VEGFR2 and the PI3-K p110 $\gamma$ . Conserved residues relative to c-Src are colored red. The p110 $\gamma$  sequence was manually aligned to c-Src using x-ray structures of the two proteins that superimpose key secondary structural elements. The VEGFR2 insert comprising residues 944–1001 is omitted.



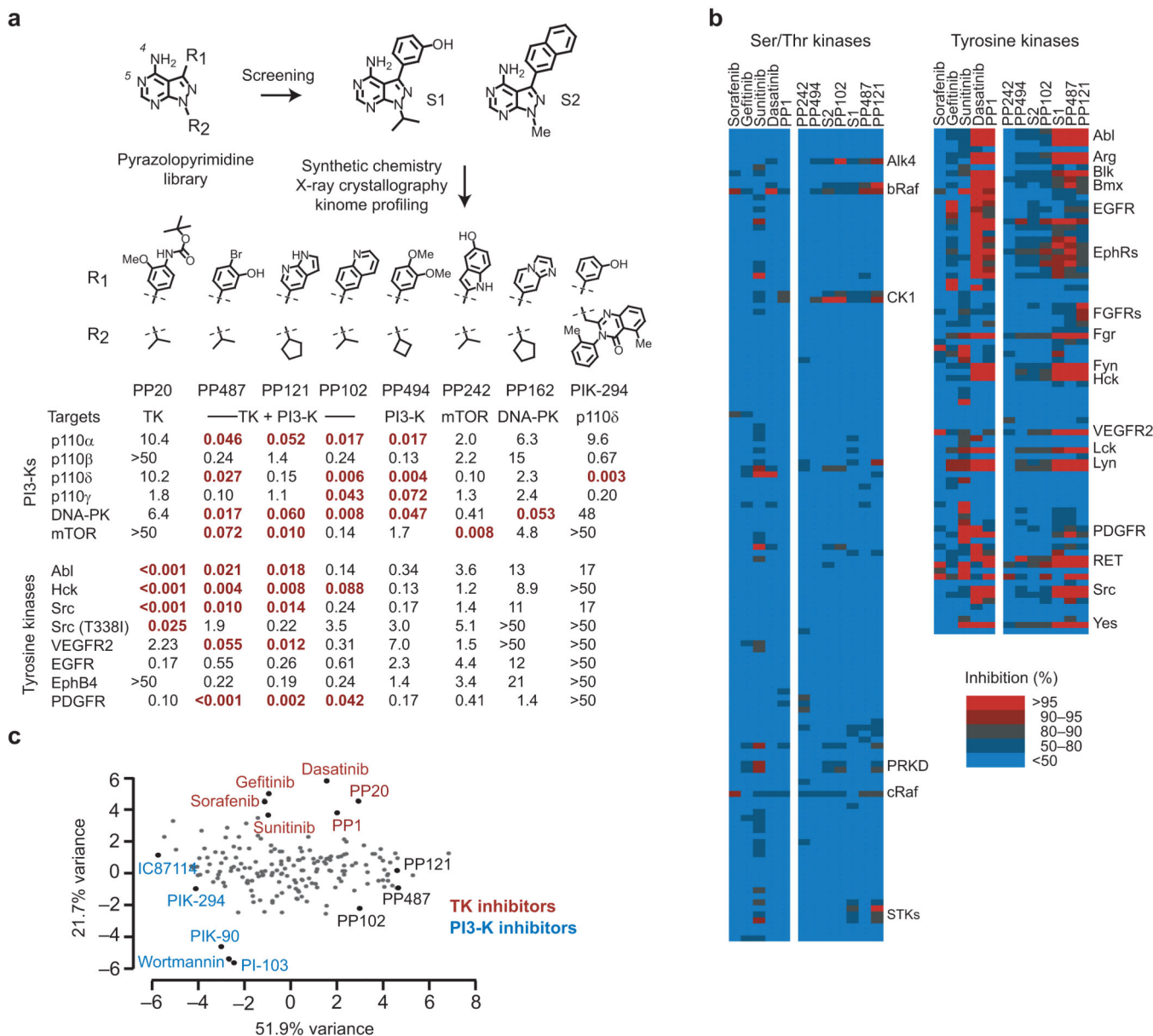


**Figure 2. Biochemical target selectivity of pyrazolopyrimidine inhibitors**

(a) Experimental strategy for the discovery of dual inhibitors, and IC<sub>50</sub> values (μM) for eight molecules tested against 14 tyrosine and phosphoinositide kinases (10 μM ATP). IC<sub>50</sub> values less than 0.1 μM are shaded red. Pyrazolopyrimidine N4 and N5, which make hydrogen bonds to the kinase, are labelled. (b) Percent inhibition of 84 tyrosine kinases (right) and 135 serine/threonine kinases (left) by 7 inhibitors from this study (right columns) and 5 reference compounds (left columns). PP inhibitors were tested at 1 μM drug and, typically, 10 μM ATP. Data from the Invitrogen SelectScreen Assay. (c) Principal component analysis of the target selectivity of 172 pyrazolopyrimidine inhibitors and 8 reference compounds. Key compounds are labelled.

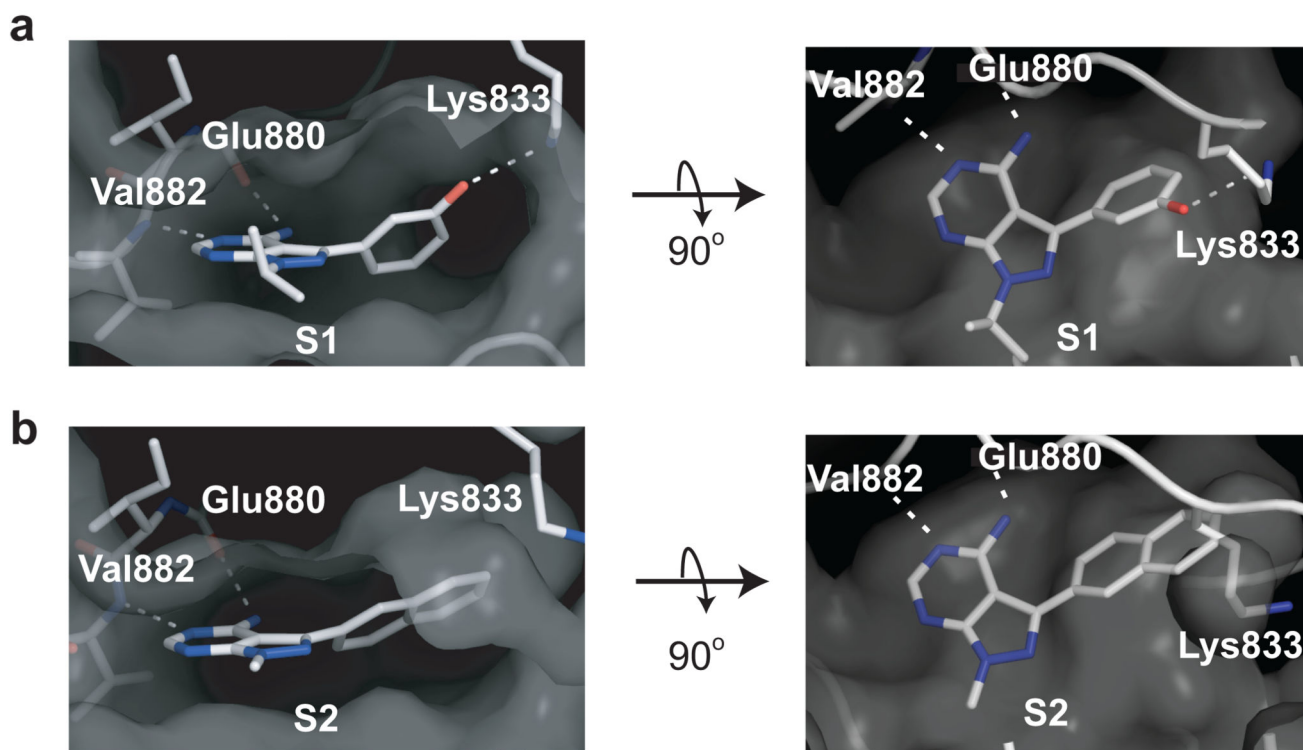


**Figure 3. Crystal structures of S1 and S2 bound to human p110 $\gamma$**   
(a) Binding mode of S1 to p110 $\gamma$ , viewed from the entrance to the ATP binding pocket (left) and above the ATP binding pocket (right). Dashed lines indicate hydrogen bonds. (b) Binding mode of S2 to p110 $\gamma$ .

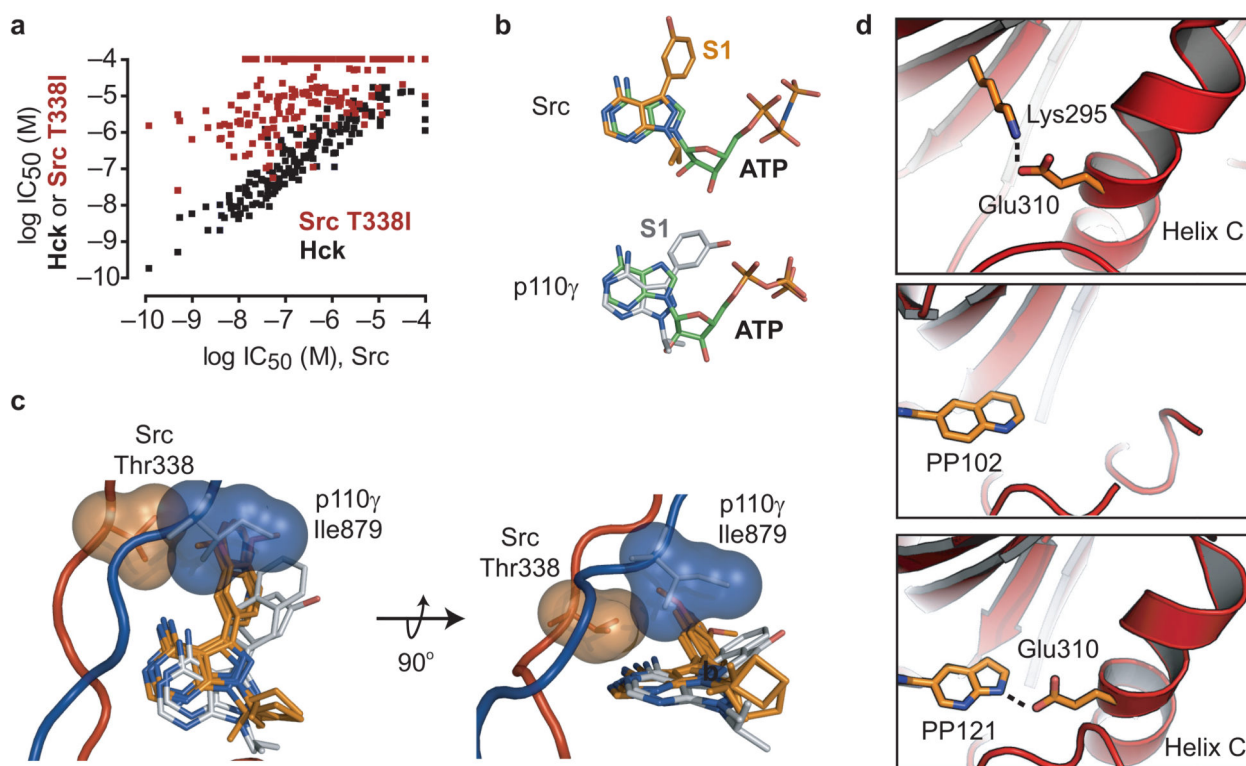


**Figure 4. Structural comparison of pyrazolopyrimidine binding to tyrosine kinases and PI3-Ks**  
 (a) Correlation between  $IC_{50}$  values for inhibitors against Src (x-axis) and either Hck or the gatekeeper mutant Src T338I (y-axis). (b) Binding orientation of S1 relative to ATP in c-Src (top) and p110 $\gamma$  (bottom). (c) Overlay of co-crystal structures of inhibitors bound to c-Src (protein colored red, drugs orange: S1, PP102, PP121, and PP494) and p110 $\gamma$  (protein blue, compounds gray: S1 and S2). The gatekeeper residues Thr338 (c-Src) and Ile879 (p110 $\gamma$ ) are highlighted. (d) (top) The catalytic lysine (Lys295) makes a hydrogen bond to Glu310 in active c-Src. (center) Helix C and Glu310 are disordered in c-Src structures containing PP102. (bottom) PP121 makes a hydrogen bond to Glu310 and orders Helix C when bound to c-Src.

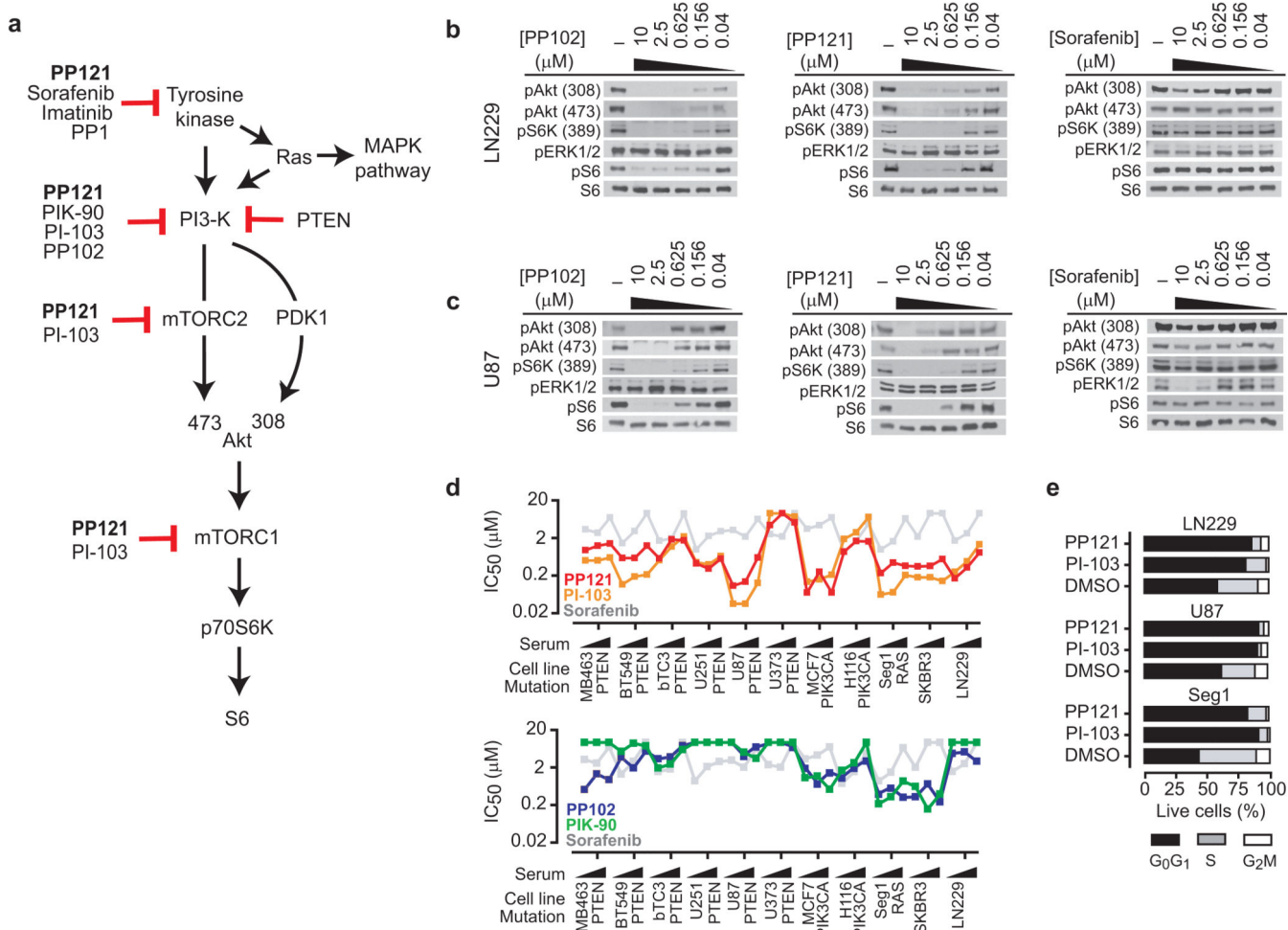


**Figure 5. PP121 directly inhibits p110 $\alpha$ /mTOR**

(a) Schematic of signaling downstream of tyrosine kinases. Not all arrows represent direct physical interactions. Drugs used in this study and their key targets are highlighted. (b)

LN229 and (c) U87 glioblastoma cells in serum (10%) were treated with PP102 or PP121 (0.040 to 10  $\mu$ M). Cells were lysed and phosphorylation of signalling proteins was probed by western blotting. pS6 (Ser235/236), pErk (Thr202/Tyr204). (d) Proliferation of tumor cells was measured following 72 h treatment with PP102, PP121, PI-103, PIK-90, or sorafenib (0.040 to 10  $\mu$ M). Each cell line was tested at three serum concentrations (0.5%, 2%, and 10%). (e) Cell cycle analysis by flow cytometry following treatment with PP121 or PI-103 (2.5  $\mu$ M) or vehicle (0.1% DMSO) for 24 h.

(a) Schematic of signaling downstream of tyrosine kinases. Not all arrows represent direct physical interactions. Drugs used in this study and their key targets are highlighted. (b) LN229 and (c) U87 glioblastoma cells in serum (10%) were treated with PP102 or PP121 (0.040 to 10  $\mu$ M). Cells were lysed and phosphorylation of signalling proteins was probed by western blotting. pS6 (Ser235/236), pErk (Thr202/Tyr204). (d) Proliferation of tumor cells was measured following 72 h treatment with PP102, PP121, PI-103, PIK-90, or sorafenib (0.040 to 10  $\mu$ M). Each cell line was tested at three serum concentrations (0.5%, 2%, and 10%). (e) Cell cycle analysis by flow cytometry following treatment with PP121 or PI-103 (2.5  $\mu$ M) or vehicle (0.1% DMSO) for 24 h.

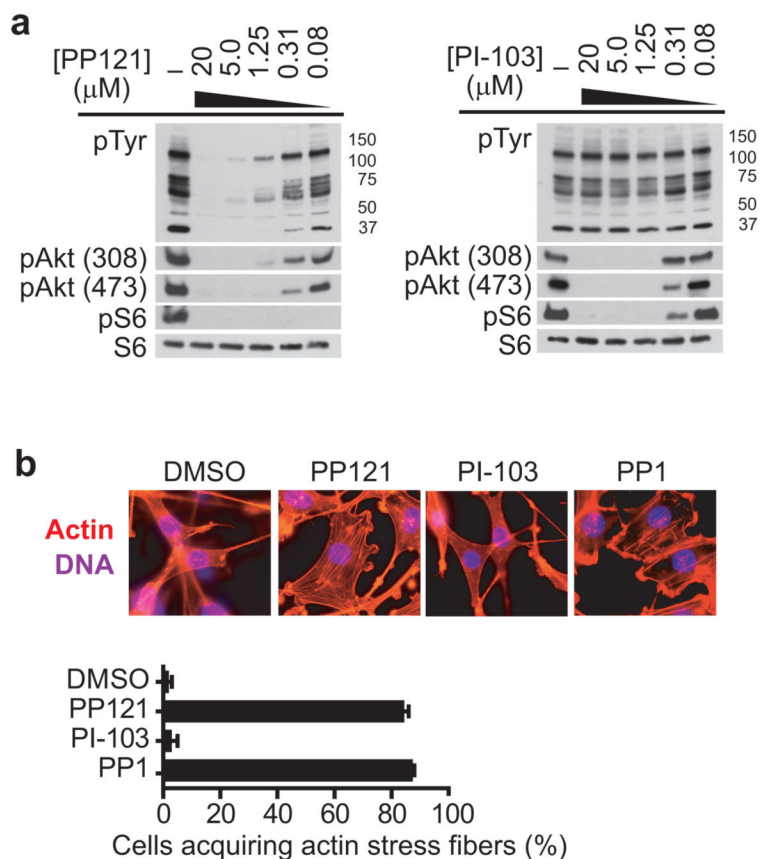


**Figure 6. PP121 directly inhibits Src**

(a) NIH3T3 cells transformed with v-Src(Thr338) were treated with the indicated concentration of each inhibitor (2 h), lysed, and blotted for indicated proteins. Molecular weights are indicated adjacent to phosphotyrosine (pTyr) blots. (b) v-Src(Thr338) transformed NIH3T3 cells were treated with the indicated inhibitors (2.5  $\mu$ M, 24 h) and then stained with FITC-phalloidin (actin) and DAPI (DNA). The percentage of cells acquiring actin stress fibers was quantitated by counting while blinded to sample identity.

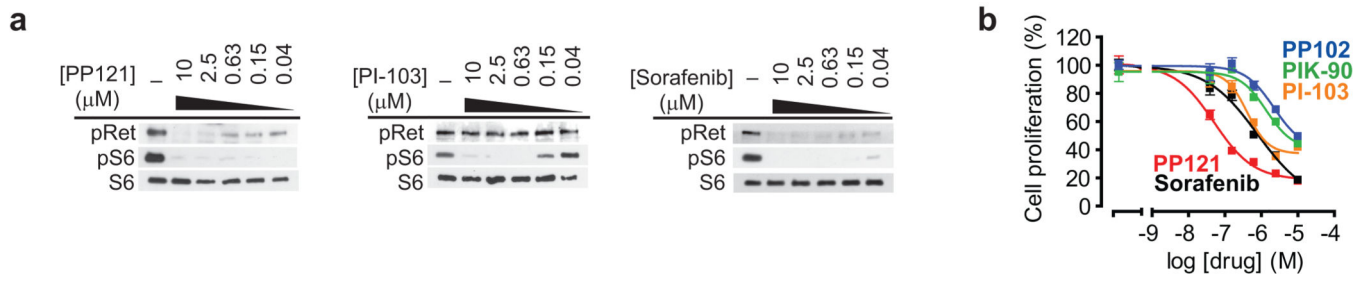


**Figure 7. PP121 directly inhibits Ret**

**(a)** TT thyroid carcinoma cells were treated with the indicated concentration of each inhibitor (2 h), lysed, and blotted for indicated proteins. pRet (Tyr905). **(b)** TT cells were treated with a dose response of each inhibitor (0.040 to 10 μM) and cell number was quantitated after 13 days. Drug was replenished every three days.

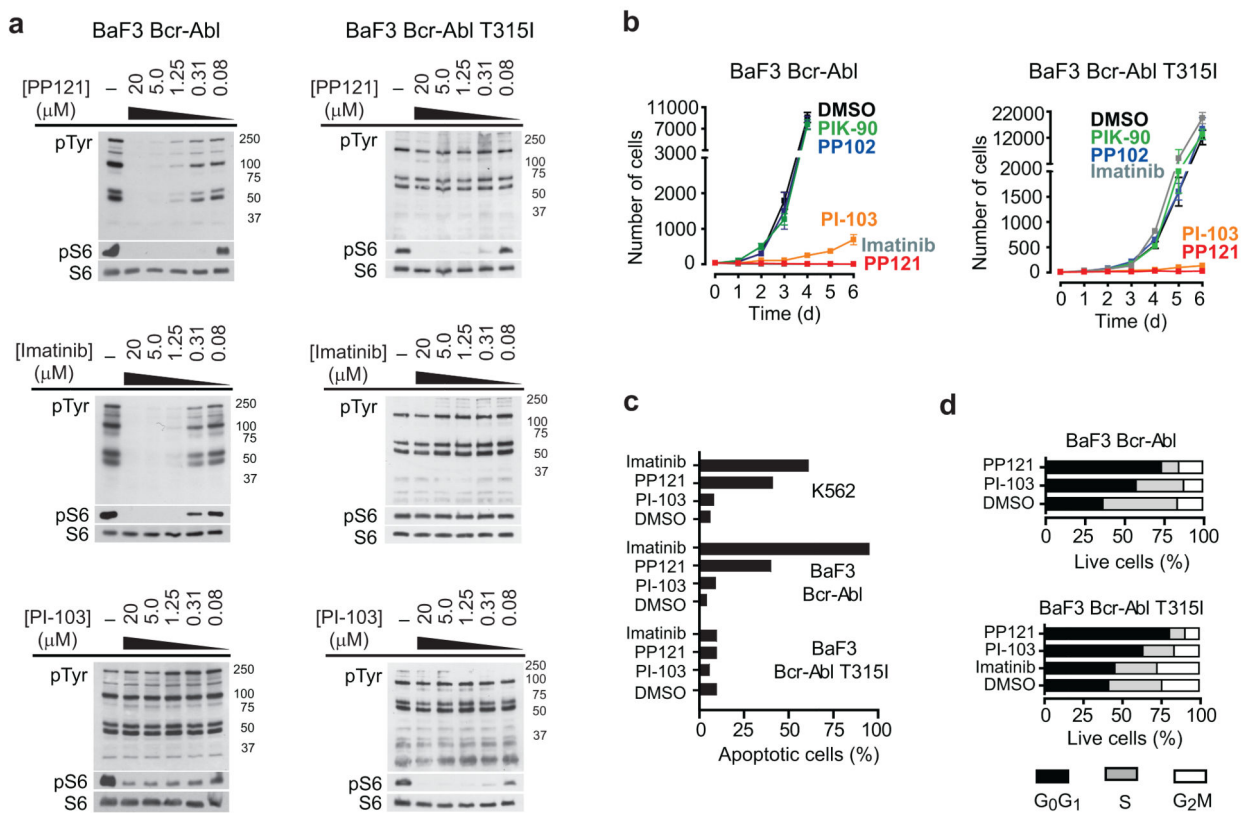


**Figure 8. PP121 reduntantly targets Bcr-Abl and PI3-K/mTOR in CML cells**

(a) BaF3 cells expressing Bcr-Abl (left column) or Bcr-Abl T315I (right column) were treated with PP121, PI-103, or Imatinib (0.080 to 20 μM) for 120 min. Cells were lysed and phosphorylation of signaling proteins was probed by western blotting. (b) Proliferation of BaF3 Bcr-Abl and BaF3 Bcr-Abl T315I cells in response to selected drugs (2.5 μM). (c) Percentage of cells undergoing apoptosis in response to drug treatment. BaF3 Bcr-Abl cells (2.5 μM, 36 h), BaF3 Bcr-Abl T315I and K562 cells (5 μM, 72 h). (d) Cell cycle analysis of live cells remaining following treatment in panel c.